

Damage assessment from curvature mode shape using unified particle swarm optimization

Bharadwaj Nanda^{*1}, Damodar Maity^{1a} and Dipak Kumar Maiti^{2b}

¹Department of Civil Engineering, Indian Institute of Technology, Kharagpur, India

²Department of Aerospace Engineering, Indian Institute of Technology, Kharagpur, India

(Received April 6, 2013, Revised February 3, 2014, Accepted June 13, 2014)

Abstract. A two-step procedure to detect and quantify damages in structures from changes in curvature mode shapes is presented here. In the first step the maximum difference in curvature mode shapes of the undamaged and damaged structure are used for visual identification of the damaged internal-substructure. In the next step, the identified substructures are searched using unified particle swarm optimization technique for exact identification of damage location and amount. Efficiency of the developed procedure is demonstrated using beam like structures. This methodology may be extended for identifying damages in general frame structures.

Keywords: damage assessment; inverse problem; curvature mode shape; stiffness reduction factor

1. Introduction

Since last three decades vibration based damage identification methods are gaining considerable attention for identifying damages in structures. These methods are based on the fact that introduction of damage decreases the stiffness of the structure, which in turn changes vibration characteristics such as natural frequency, mode shape and damping of the structure. The main advantage associated with these methods lie in the global nature of vibration characteristics, due to which it is able to identify damages located in hidden or internal areas, where visual inspection is difficult to conduct.

Thatoi *et al.* (2012) provides a comprehensive review of recent developments of vibration based damage identification techniques. In a damage identification problem usually two objectives are attained; (i) finding the location of the damage and then (ii) estimating its severity. To attend these objectives, most of the vibration based damage identification procedures follow more or less same approach. Firstly, a mathematical relationship is constructed between damage condition and changes in structural response due to this. Then an objective function is defined using vibration parameters identified from modal testing and corresponding values calculated from finite element simulation. Finally, an inverse problem is formulated using a suitable optimization technique to

*Corresponding author, Research Scholar, E-mail: bharadwajnanda@gmail.com

^aProfessor, E-mail: dmaity@civil.iitkgp.ernet.in

^bProfessor, E-mail: dkmaiti@aero.iitkgp.ernet.in

optimize this objective function by changing the damage locations and severity.

As the mathematical relationship between structural vibration response and the location and extent of damage is quite complex, nowadays computational intelligence techniques, such as genetic algorithm (Maity and Tripathi 2005, Mehrjoo *et al.* 2013), artificial neural network (Maity and Saha 2004, Bakhary *et al.* 2010, Sahoo and Maity 2007, Vallabhaneni and Maity 2011) and swarm based intelligence techniques such as ant colony optimization (Majumdar *et al.* 2012, Yu and Xu 2011) and particle swarm optimization (Nanda *et al.* 2012, Sayedpoor 2012) are widely employed to solve such problems. To construct suitable objective function for this purpose, most of the authors used natural frequency, mode shape or their derivatives. It is a well-known fact that, the complexity of damage identification algorithm increases with the dimension of search space or number of unknowns. In this context, curvature mode shapes (Pandey *et al.* 1991, Tripathi and Maity 2004, Al-Ghalib *et al.* 2011, Chandrashekhar and Ganguli 2009, Zhang *et al.* 2011) provide a visual indication of damaged members, as maximum change in curvature mode shapes are localized to the damaged regions. This property of curvature mode shapes can suitably be used to construct an improved two step damage identification procedure. In the first step, substructures containing the probable damage location can be visually identified by observing the changes in curvature mode shapes. In the next step, the identified substructures can be searched using optimization technique for exact identification of damage location and its amount. This two-step procedure not only reduces the complexity of the problem but also improves the accuracy of prediction.

Particle swarm optimization (PSO) (Kennedy Eberhart 1995) is a swarm based computational intelligence technique, well known for its ability to find the global optima quickly even in case of complex engineering problems. However in its original form, PSO has low exploration ability due to which, the particles may converge to some local optima and thereby it may end up in prediction of wrong results. Many alternations and variations are proposed to the original PSO algorithm to improve its efficiency (Banks *et al.* 2007, 2008). Moreover, from literatures it is found that refined versions of PSO algorithm are generally used for solving damage assessment problems (Perera *et al.* 2010, Liu *et al.* 2011, Nanda *et al.* 2012, Kang *et al.* 2012, 2013, Guo and Li 2013). Here, an improved version of the PSO technique called unified particle swarm optimization (UPSO) (Parsopoulos and Vrahatis 2010), which is well known for providing better exploration and exploitation capability simultaneously, is proposed for solving such problem. In this study, a numerical procedure is developed which can detect and assess the state of damage in a structure using curvature damage factor and unified particle swarm optimization. Numerical models of undamaged and damaged structures are simulated for estimation of damaged curvature damage factor (CDF). Several numerical simulations are carried out to demonstrate the efficacy of the proposed procedure

2. Theory and formulation

A brief review of theoretical formulations for modeling the undamaged and damaged structures, procedure for damage identification and brief description of UPSO algorithm is presented in this section.

2.1 Damage formulation

For the present study, damage is assumed as reduction in stiffness without any appreciable changes in mass of the structure. This is usually incorporated by using a parameter called, “Stiffness Reduction Factor (SRF)”. The SRF value corresponds to the factor by which stiffness of undamaged element is reduced in damaged element. It ranges from 0, 1 where 0 signifies no damage in the element and 1 means the stiffness is completely lost for the element. Mathematically

$$[k_{d,i}] = (1 - \beta_i)[k_i] \tag{1}$$

Where β_i denotes the stiffness reduction factor, $[k_i]$ and $[k_{d,i}]$ denotes the undamaged and damaged elemental stiffness matrices for i^{th} element. Considering $[K_d]$ and $[M]$ as the global stiffness and mass matrix for the damaged element, the eigen equation for the damaged structure can be written in the form:

$$[[K_d] - \omega_{di}^2 [M]]\{\phi_d^i\} = \{0\} \tag{2}$$

Where, ω_{di} and ϕ^i represents the i^{th} natural frequency and mode shape respectively.

2.2 Curvature damage factor

Curvature is the rate of change of slope per unit length. Mathematically it is given by

$$\text{Curvature} = \frac{1}{R} = \frac{M}{EI} = \frac{\partial^2 v}{\partial x^2} \tag{3}$$

From the displacement mode shape, the curvature mode shape may be obtained by central difference approximation as

$$v_i'' = \frac{v_{i+1} - 2v_i + v_{i-1}}{h^2} \tag{4}$$

Where h is the length of the element and v_i 's are the transverse displacement. Curvature damage factor (CDF) is defined as “mean of the absolute difference between modal curvatures of undamaged and damaged structure”. Mathematically

$$CDF = \frac{1}{N} \sum_{n=1}^N |v_{ui}'' - v_{di}''| \tag{5}$$

Where, N is the number of modes considered for damage identification, v_{ui}'' and v_{di}'' denotes the curvature mode shapes for the undamaged and damaged structures respectively for the i^{th} node.

2.3 Sub-structural Identification

The number of unknown parameters for damage identification increases with the increase in the size of the structure. This increases the complexity of the problem due to which it becomes computationally expensive and sometimes practically impossible to identify damages in large structures. However, in most of the cases, it is expected that the damages are occurred in some critical locations of the structure. The damage identification may be carried out only at those

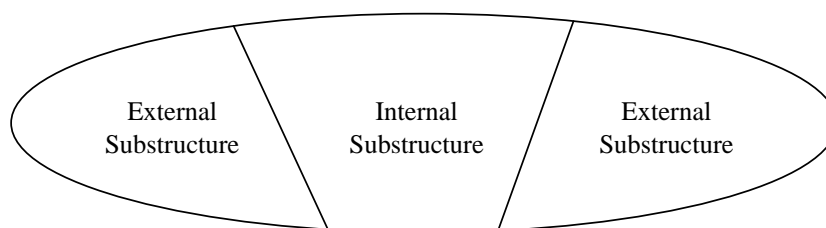


Fig. 1 Substructuring for local identification

locations which can ease the complexity of the problem to a great extent. Due to its simplicity, the sub-structuring method proposed by Yun and Bahng (2001) is used for the present study. Here, the substructure to be identified is called the internal substructure and the others are called the external substructures, as shown in Fig. 1. As maximum changes in curvature mode shapes are localized to the damaged regions, appropriate substructure for damage identification is selected by visual identification. Then, these identified substructures are searched using some optimization technique for assessment of exact damage location and amount.

2.4 Unified particle swarm optimization

The particle swarm optimization (PSO) algorithms, first proposed by Kennedy and Eberhart (1995), are inspired by “swarm behavior”, the collective motion of insects and birds trying to reach an unknown destination. In a flock of birds, each bird looks in a specific direction and then, when communicating together, they identify the bird present at the best position at a particular time. Accordingly, each bird moves towards the best bird with a velocity proportional to its current position. Each bird, then, searches for a new direction from its new local position and the process repeats until the flock reaches a desired destination. Hence, the entire process involves both social interaction and intelligence so that birds learn from their own experience and also from the experience of others around them. This process of social interaction and social learning is achieved by the formation of neighborhoods. Two general types of neighborhoods has been defined as, the global best (Where each particle shares information with each member of the swarm) and the local best (Where each particle shares information with its immediate neighbors according to certain topology rules).

The global variant of PSO converges faster since all particles are attracted by the same best position and hence promotes exploitation. On contrary, this too makes global variant more prone to get trapped into a local maximum or minimum. On the other hand, the local variant has better exploration properties, since the information regarding the best position of each neighborhood is gradually communicated to the rest of the particles through their neighbors. Thus, the attraction towards a specific point is weaker, preventing the swarm from getting trapped in suboptimal solutions. For an effective optimization, it is desirable to have good exploration ability during early stages of the optimization, whereas during later stage it should have good exploitation ability. Unified particle swarm optimization (UPSO) is a scheme to harness these abilities by combining both global and local variants of PSO algorithms respectively (Parsopoulos and Vrahatis 2010) using a factor u that balances the influence of the global and local search directions.

Numerically, for a swarm of P -particles in S -dimensional search space, let G_{ij}^{t+1} and L_{ij}^{t+1} denotes the velocity update of i^{th} particle in global and local variants of PSO respectively for $(t + 1)^{th}$

iteration as given by

$$G_{ij}^{t+1} = \chi \left[v_{ij}^t + c_1 r_1 (pbest_{ij} - x_{ij}^t) + c_2 r_2 (gbest_{ij} - x_{ij}^t) \right] \quad (6)$$

and

$$L_{ij}^{t+1} = \chi \left[v_{ij}^t + c_1 r_3 (pbest_{ij} - x_{ij}^t) + c_2 r_4 (lbest_{ij} - x_{ij}^t) \right] \quad (7)$$

Where, *pbest*, *gbest* and *lbest* in above equations denotes the best position explored by individual particle, any particle in the swarm and in the neighborhood of individual swarm respectively. χ denotes the constriction factor whose value equals to 0.72984. Further, all *c* terms denote the acceleration terms and all *r* terms correspond to random numbers between [0,1]. Combining Eqs. (6) and (7), the aggregate velocity of the search directions is defined as

$$V_{ij}^{t+1} = u \cdot G_{ij}^{t+1} + (1 - u) \cdot L_{ij}^{t+1}, \quad u \in [0,1] \quad (8)$$

Where, *u* is called unification factor and the value of *u* increases linearly from 0 to 1 throughout the iterations. The new position of the particles for (*t* + 1)th iteration is

$$x_{ij}^{t+1} = x_{ij}^t + V_{ij}^{t+1}, \quad \forall i \in P \text{ and } \forall j \in S \quad (9)$$

2.5 Damage identification procedure

A two stage damage assessment procedure is developed based on the outlined theoretical formulations. Maximum changes in curvature mode shapes are localized to the damaged regions. Hence, the substructures containing the probable damage location is visually identified by comparing curvature mode shapes of numerical undamaged structure and measured damaged structure. In the next step, the probable damaged substructures are searched using UPSO algorithm for locating and quantifying the actual damaged elements. The sum of differences between the measured CDF value and the numerical CDF value is used for constructing objective function. Mathematically

$$F = \sum_{i=1}^N |CDF_m - CDF_c| \quad (10)$$

Where, *CDF_m* denotes the CDF value measured for the damaged structure and *CDF_c* denotes the CDF value estimated for the structure for a probable damage scenario generated during the process of optimization. The CDF value for the actual structure is estimated by experimentally. Then the optimization technique is employed to search some pairs of SRF value for which the CDF value for the numerical structure exactly match with that of the measured CDF value. The SRF values for which this match occurs provides the actual damage scenario. Fig. 2 shows flow chart for the two stage procedure for structural damage assessment using curvature damage factor.

3. Results and discussions

3.1 Damage identification in a simply supported beam

A steel beam with simply support conditions is considered for the demonstration purpose. The length of the beam is considered as 1000 mm, cross sectional area as 360 mm^2 , moment of inertia as 6750 mm^4 . The Young's modulus and material density of the beam element is considered as 210 GPa and 7800 kg/m^3 respectively. The beam is modeled with 20 equal Euler-Bernoulli beam elements. Fig. 3 represents the sketch of the beam used for finite element model. Modal analysis of the beam is carried out by generalized eigen value analysis. The damage condition is

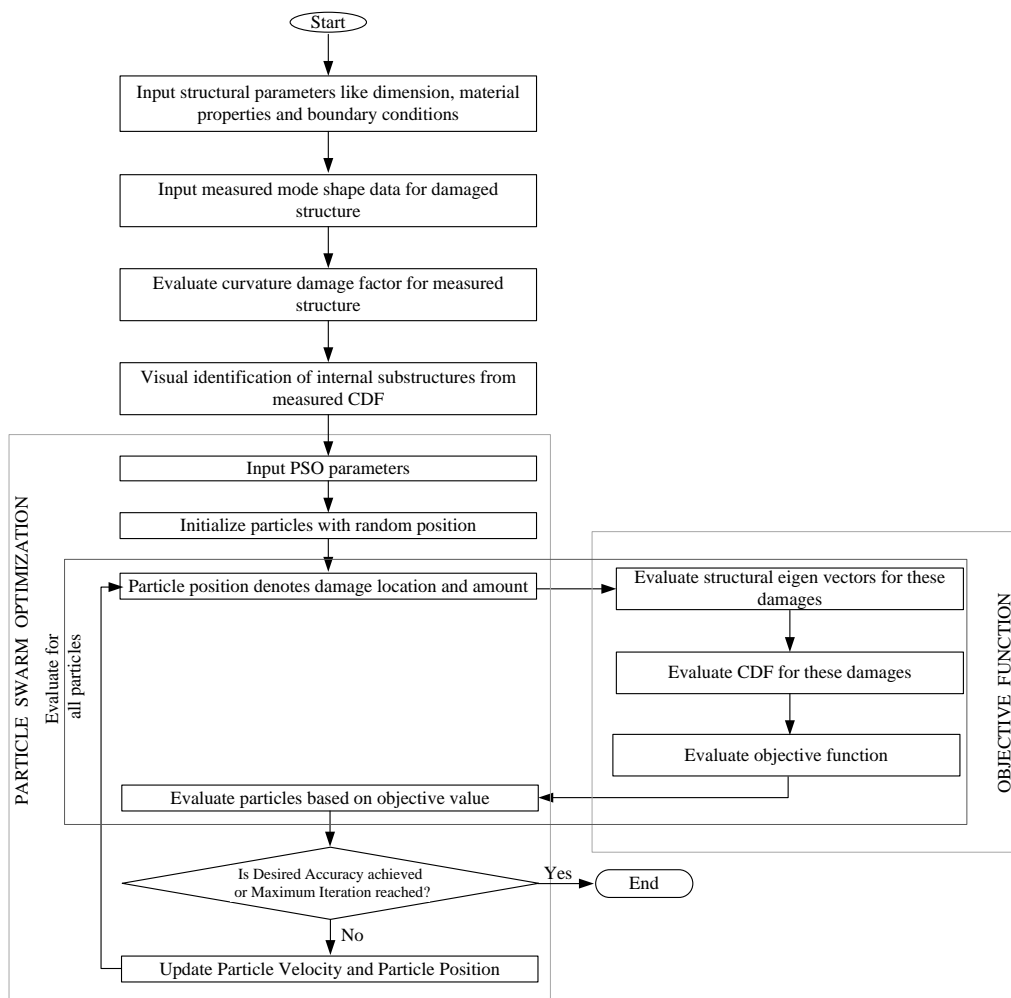


Fig. 2 Two stage procedure for structural damage assessment using curvature damage factor

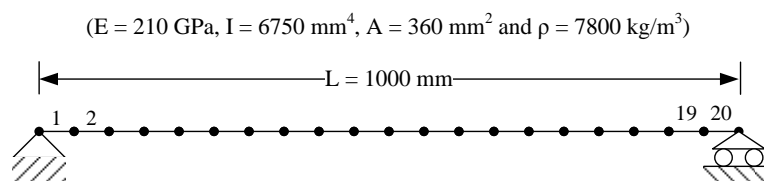


Fig. 3 Finite element model of simply supported steel beam

simulated by reducing stiffness of the entire beam element by an amount proportional to SRF. Fig. 4 represents first three mode shapes and corresponding natural frequencies of the numerical beam.

3.1.1 Single element damage identification

For the demonstration purpose, a single element damage problem with 15% damage at element 5 is considered. For numerical simulation purpose the stiffness of element 5 is reduced by 15% (SRF = 0.15). Curvature mode shapes are calculated for both undamaged and damaged structure and then the changes in curvature mode shapes are calculated as shown in Fig. 5. Normally distributed random noise up to 10% standard deviation is added to numerically estimated curvature mode shapes to simulate real experimental conditions. In general, lower modes of curvature mode shapes provide better visualization of damaged elements than higher modes. Whereas, it is observed from Fig. 5 that, the magnitude of changes in curvature mode shapes is less in lower modes than those of the higher modes. Hence for a better visualization of lower modes, the changes in curvature mode

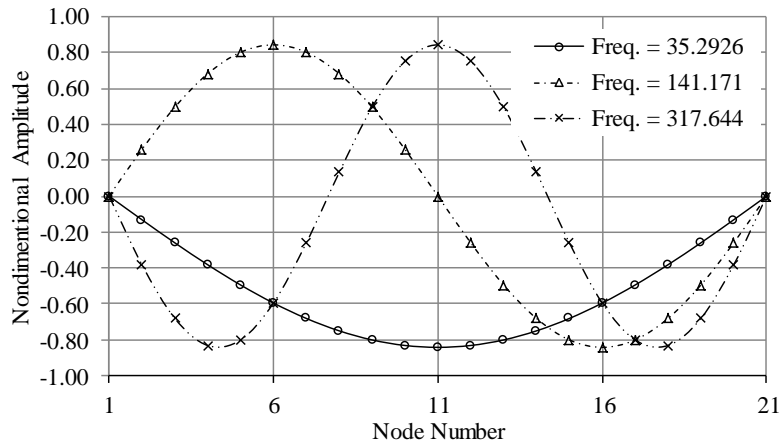


Fig. 4 First three mode shapes of the simply supported beam

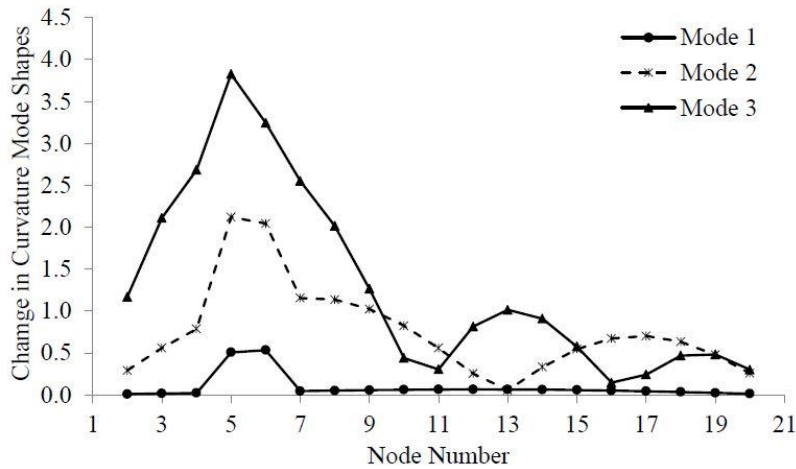


Fig. 5 Changes in first three curvature mode shapes for single element damage

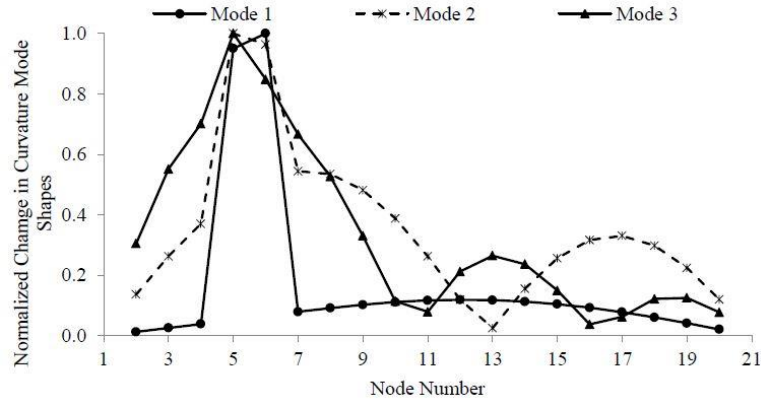
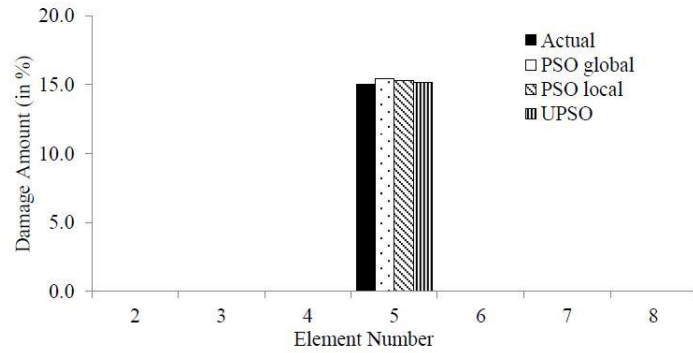
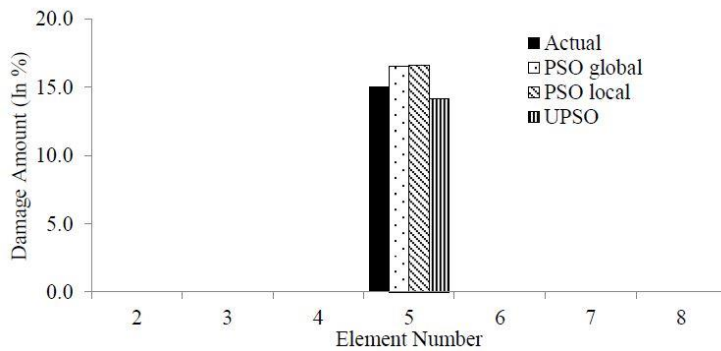


Fig. 6 Normalized changes in curvature mode shapes for single element damage



(a) Damage identification with 5% noise in CDF value



(b) Damage identification with 10% noise in CDF value

Fig. 7 Single element damage identification result

shapes for all these modes are normalized to unit value as is shown in Fig. 6 wherein it is observed that, the maximum change in curvature mode shapes are localized within nodes 5 and 6, corresponding to element 5. This implies that element 5 has the maximum probability of being damaged. Hence elements near to element 5 should be included in internal sub-structure. Apart from these elements, few minor peaks are also observed in other nodes such as, node 13 and node

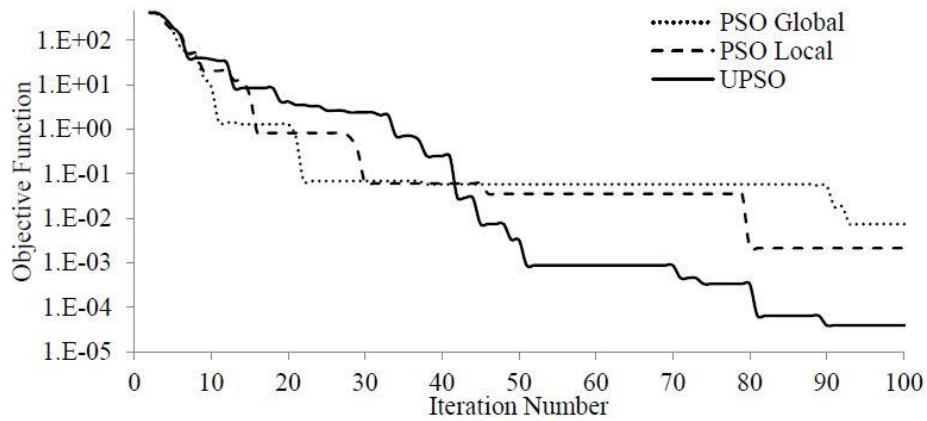


Fig. 8 Progress of objective function with iteration for single element damage case

17. Logically elements connected to these nodes should be included in internal sub-structure, as the exact damage scenario is still unknown. Considering all these aspects the internal substructures can effectively be reduced to elements [4, 5, 6, 12, 13, 17 and 18].

The actual damaged element and corresponding damage percentage are estimated by employing UPSO algorithm. A comparison is made among UPSO with global and local variants of standard PSO algorithms to understand their performance in solving present problem. The maximum swarm size is considered as 30 and the maximum iteration is limited to 1000 for both USPO, global and local variants of PSO. Each experiment is executed for five times and the damage scenario which corresponds to minimum objective function is considered as actual damage scenario. First three modes are considered for damage identification in this case. The uncertainties associated in test results are simulated numerically by adding up to 10% normally distributed random noise in analytical CDF value. Fig. 7 presents the results of damage identification considering noise in CDF as 5% and 10%.

It is observed from Fig. 7 that, performance of this two-way procedure is quite impressive. Further the effect of addition of noise on the algorithm is not so significant. In other words, the procedure has a good immunity to the noise. Furthermore, in comparison to UPSO, the performances of other two algorithms are poor. In particular, when the noise level in estimation of CDF is 10% it is observed that the other two algorithms take longer time to converge. For a clear comparison on convergence of the three algorithms, the progress of objective function for the problem with noise free CDF value is provided in Fig. 8. It is observed that, the UPSO based algorithm converges faster than other two. In addition, few more single element damage assessment problems are simulated considering 5%, 10%, 20% and 30% damages at elements 5 and 10 respectively. These problems and corresponding results are summarized in Table 1.

For evaluating the performance of the present algorithm with severely noisy environment, up to 20% noise is added to the numerically simulated CDF value. A study is carried out to evaluate the robustness of the proposed algorithm with different noise conditions. Each experiment is conducted for five times considering different starting seeds and different noise amounts. These are then solved using UPSO and global and local variants of standard PSO algorithms. The performances of these algorithms are measured in terms of *success rate*, *mean error* and *standard deviation* in damage identification results. *Success rate* indicates ratio of number of times the algorithm is able

Table 1 Single element damage identification results

Noise Level	Damage Id	Actual Damage	Global PSO			Local PSO			UPSO		
			Success Rate	Error in Damage Identification (in %)		Success Rate	Error in Damage Identification (in %)		Success Rate	Error in Damage Identification (in %)	
				Mean	Std. Dev.		Mean	Std. Dev.		Mean	Std. Dev.
5% Noise	C1	5% @5	0.60	1.60	0.10	1.00	0.20	0.10	1.00	0.20	0.09
	C2	10% @5	1.00	0.50	0.05	1.00	0.40	0.04	1.00	0.30	0.05
	C3	20% @5	0.60	0.05	0.29	1.00	0.30	0.18	1.00	0.00	0.23
	C4	30% @5	1.00	0.43	0.49	1.00	0.57	0.45	1.00	0.50	0.45
	C5	5% @10	0.40	2.00	0.01	0.80	1.20	0.16	1.00	0.20	0.15
	C6	10% @10	0.60	0.50	0.17	1.00	0.20	0.15	1.00	0.10	0.16
	C7	20% @10	0.40	0.95	0.58	0.80	1.95	0.32	1.00	1.30	0.22
	C8	30% @10	0.80	1.17	0.81	1.00	0.20	0.49	1.00	0.17	0.48
10% Noise	C1	5% @5	0.60	2.20	0.13	0.80	0.20	0.18	1.00	0.00	0.16
	C2	10% @5	1.00	0.60	0.52	1.00	0.60	0.52	1.00	0.50	0.47
	C3	20% @5	0.80	0.50	0.68	1.00	0.00	0.66	1.00	0.15	0.63
	C4	30% @5	1.00	0.33	1.19	1.00	0.60	1.20	1.00	0.47	1.15
	C5	5% @10	0.00*	-	-	0.80	0.20	0.17	1.00	0.60	0.19
	C6	10% @10	0.40	0.70	0.17	1.00	1.50	0.26	1.00	1.40	0.24
	C7	20% @10	0.60	1.95	0.84	1.00	1.50	0.56	1.00	1.35	0.57
	C8	30% @10	0.80	0.80	0.52	0.60	0.93	0.71	1.00	0.33	0.66
15% Noise	C1	5% @5	0.80	1.40	0.34	0.80	0.20	0.35	1.00	0.60	0.30
	C2	10% @5	0.80	0.60	0.42	1.00	0.70	0.52	1.00	1.20	0.57
	C3	20% @5	1.00	0.80	1.20	1.00	0.60	1.21	1.00	0.35	1.12
	C4	30% @5	0.80	0.07	0.91	1.00	1.63	1.06	1.00	1.73	0.98
	C5	5% @10	0.40	0.60	0.13	0.60	4.20	0.30	0.60	1.80	0.22
	C6	10% @10	0.20	5.90	0.00	1.00	0.40	0.67	1.00	0.50	0.67
	C7	20% @10	0.40	0.70	0.96	1.00	2.20	0.71	1.00	0.95	0.17
	C8	30% @10	0.40	2.37	0.89	1.00	1.83	1.38	1.00	1.77	1.37
20% Noise	C1	5% @5	1.00	1.20	0.41	1.00	2.00	0.40	1.00	1.85	0.37
	C2	10% @5	1.00	0.30	0.86	1.00	0.70	0.72	1.00	0.80	0.75
	C3	20% @5	1.00	0.20	2.18	1.00	0.20	1.92	1.00	0.20	1.90
	C4	30% @5	1.00	2.77	2.20	1.00	2.97	2.00	1.00	2.33	2.00
	C5	5% @10	0.60	2.80	0.15	0.80	2.40	0.19	1.00	2.40	0.16
	C6	10% @10	0.20	1.60	0.00	0.80	0.40	0.56	1.00	0.60	0.53
	C7	20% @10	0.40	0.30	0.78	0.80	0.45	1.25	1.00	0.00	1.10
	C8	30% @10	0.60	5.10	0.51	1.00	2.00	1.46	1.00	1.73	1.54

*Damage is detected at element number 9

to identify correct damaged element to total number of experiments carried out. A success value equals to 1 means the selected algorithm could able to identify the correct damaged element for all runs (five for the present case) where as a value equals to 0 means it failed to identify the correct damaged element for all runs. It may be observed from the Table 1 that, for most of the cases,

UPSO algorithm is able to achieve the *success rate* of 1.0 which indicates its superior performance than other two variants of standard PSO.

Further, the error in damage identification is measured for evaluating the robustness of the present algorithm. The error in damage assessment is measured in percentages from the difference of actual and predicted amounts of damage considered for simulation study and by dividing it with actual damage amount considered. The error is calculated for different runs are then averaged to obtain the *mean error in damage identification*. A lower value of *mean error* signifies better damage quantification results. Finally, the robustness of the damage quantification results are measured in terms of *standard deviation in damage identification* values. The *standard deviation* value signifies the variation of damage quantification result from the mean values. A *standard deviation* value provides a direct measure for robustness of the algorithm. It is clearly observed from the Table 1 that, the proposed method is able to identify the damaged element and damage percentage accurately with significant precession. It may be observed from Table 1 that, the maximum amount of error associated with damage assessment is 2.33% for C4 damage condition and 2.40% for C5 damage condition for a noise level of 20% which is quite acceptable considering the amount of noise associated with the CDF values. Moreover, the maximum value of *standard deviation* associated with the damage identification results is 2.0 for C4 damage condition for a noise level of 20%. This signifies the algorithm is robust enough to solve damage identification problems for the considered noise levels.

3.1.2 Multiple element damage identification

To verify the practicability of the proposed algorithm in multiple damage identification case, the simple support beam used in section 3.1.1 is considered. Multiple damage case is simulated by reducing stiffness of 5th and 15th element simultaneously by 10 % and 15 % respectively. Normally distributed random noise up to 10% standard deviation is added to numerically estimated curvature mode shapes to simulate real experimental condition. Similar to section 3.1.1, the curvature mode shape changes are normalized to unit value, as shown in Fig. 9, to estimate the internal substructure for second step of damage identification.

It is observed from Fig. 9 that, maximum changes in curvature mode shapes are localized at element 14 to 16. Another peak is also observed at elements 4 to 7. Hence, considering the aspects

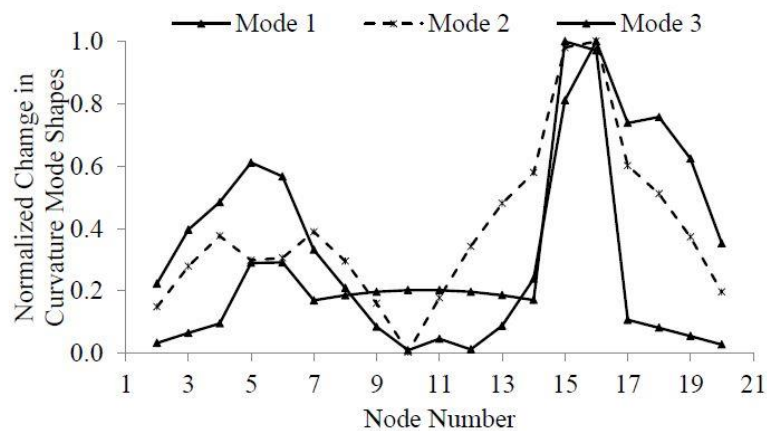


Fig. 9 Normalized changes in curvature mode shapes for double damage case

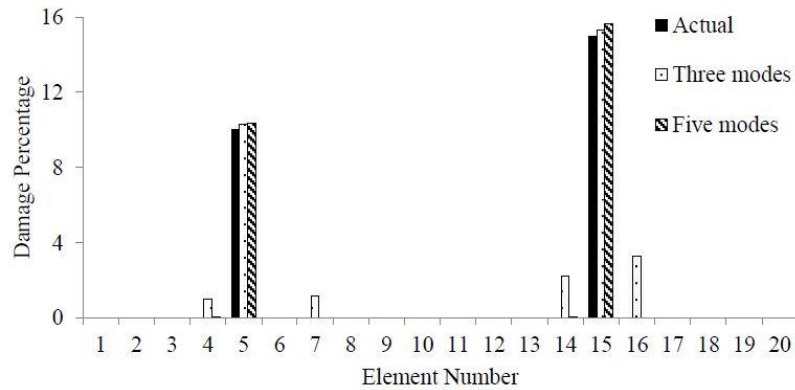


Fig. 10 Result of multiple element damage identification

Table 2 Damage identification results for double element damage

Damage Cases	Actual Damage		Damage Identification using 3 Mode			Damage Identification using 5 Mode		
	Element	Amount	Identified Damage	Error (in %)	Std. Dev.	Identified Damage	Error (in %)	Std. Dev.
10% Noise in CDF Values								
D ₁	5	5	4.79	4.20	0.04	4.93	1.31	0.01
	10	5	4.73	5.48	1.41	5.07	1.34	0.01
D ₂	5	10	10.59@3*	-	-	9.81	1.87	1.11
	10	20	20.18	0.88	0.46	19.71	1.47	0.04
D ₃	5	20	19.54	2.29	0.63	19.32	3.41	0.03
	10	20	18.40	8.00	4.34	19.44	2.82	0.02
D ₄	5	20	19.24	3.82	0.38	19.75	1.26	0.14
	10	30	29.03	3.24	0.06	29.52	1.59	0.03
20% Noise in CDF Values								
D ₁	5	5	5.16	3.20	0.12	4.82	3.60	0.30
	10	5	5.35	7.00	0.20	4.79	4.20	0.43
D ₂	5	10	10.85	8.50	0.11	9.41	5.90	0.94
	10	20	21.60	8.00	0.64	19.02	4.90	0.88
D ₃	5	20	20.01	0.05	0.94	20.21	1.05	0.95
	10	20	20.19	0.95	2.56	20.51	2.55	1.37
D ₄	5	20	19.99	0.05	2.02	19.43	2.85	1.14
	10	30	30.70	2.33	3.69	29.14	2.87	1.59

*Detected damage is 10.59% at element number 3.

described in previous section, suitable internal substructure for second step of damage identification can be considered as [4, 5, 6, 7, 14, 15 and 16]. As from previous study, UPSO is found to be the best performing algorithm; the same is used for solving the present problem. All the parameters required for UPSO algorithm is kept similar to the previous section. First three and first five modes of vibration are used for damage identification. The results of damage assessment are shown in Fig. 10.

It is observed from Fig. 10 that, though the proposed procedure is able to detect damaged member correctly with first three modes, but it detects few false damage also. However, using first five curvature modes the correct damaged scenario can be achieved without any false damage. Few more double element damage identification cases are simulated as shown in Table 2. Random noise up to 20% is added to curvature mode shape for demonstration purpose. It is observed from the table that, using first three curvature mode shapes it is possible to detect and quantify the damage properly for most of the cases. However, for accurate determination of damaged element with damage extent, first five frequencies would be a better choice. Further, the number of false damage significantly reduces if first five curvature mode shapes are used for assessment purpose. By using first three modes, the algorithm is unable to identify correct damaged member for the case D₃. But by using first five modes, it is possible to locate all damaged elements properly in all considered cases. Similarly, it is observed that, the *mean error in damage identification* and *standard deviation* associated with the damage identifications are quite less when first five modes are considered for damage identification. This proves the robustness of the present damage identification algorithm.

3.2 Damage identification in a Cantilever beam

A steel cantilever beam with dimensions similar to the simply supported beam taken in previous section is considered. Fig. 11 represents the sketch of the beam used for finite element simulation. Fig. 12 represents first three mode shapes and corresponding natural frequencies of the beam.

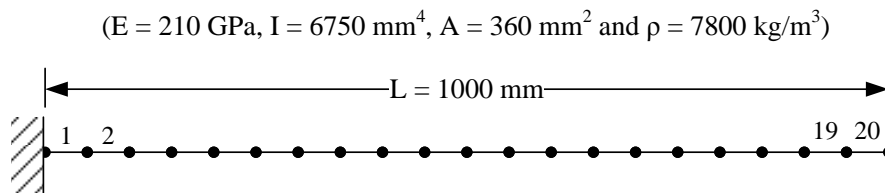


Fig. 11 Finite element model of cantilever steel beam

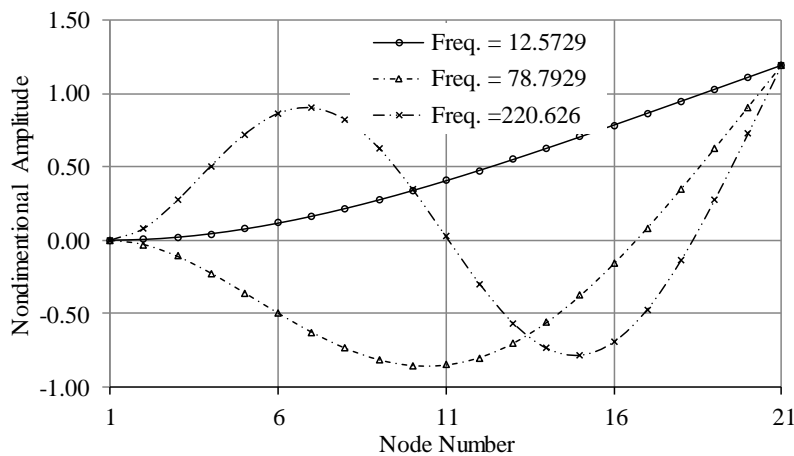


Fig. 12 First three mode shapes of the cantilever beam

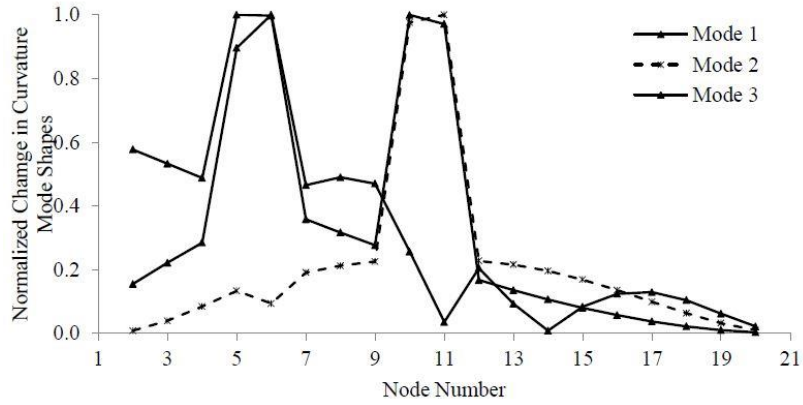


Fig. 13 Normalized changes in curvature mode shapes for a double damage case

Table 3 Damage identification results for cantilever beam

Damage Cases	Actual Damage		Damage Identification using 3 Mode			Damage Identification using 5 Mode		
	Element	Amount	Identified Damage	Error (in %)	Std. Dev.	Identified Damage	Error (in %)	Std. Dev.
10% Noise in CDF Values								
E1	5	5	5.46	9.20	0.00	4.94	1.20	0.01
E2	8	10	11.29 & 9.41@6*	-	-	9.93	0.70	1.19
E3	10	15	15.72	4.80	0.01	15.59	3.93	0.96
E4	10	30	30.11	0.37	1.32	28.39	5.37	0.08
E5	6	10	9.39	6.10	0.01	9.63	3.70	0.00
E6	14	10	9.51	4.90	0.02	9.78	2.20	0.00
E7	5	5	5.42	8.40	0.00	5.08	1.60	0.02
E8	12	20	20.73	3.65	0.01	21.25	6.25	0.00
E7	5	5	5.08	1.60	0.12	4.96	0.80	0.04
E8	10	20	20.79	3.95	0.42	19.19	4.05	0.03
E8	5	20	19.48	2.60	0.12	20.26	1.30	0.06
E8	15	20	19.71	1.45	1.11	20.30	1.50	0.81
20% Noise in CDF Values								
E1	5	5	5.33	6.60	0.43	4.80	4.00	0.11
E2	8	10	9.90	1.00	0.65	10.02	0.20	0.89
E3	10	15	14.71	1.93	1.71	15.10	0.67	0.81
E4	10	30	31.73	5.77	2.58	29.86	0.47	2.25
E5	6	10	9.24	7.60	0.75	9.63	3.70	0.40
E6	14	10	9.26	7.40	0.11	9.78	2.20	0.03
E6	5	5	5.13	2.60	0.79	5.09	1.80	0.07
E6	12	20	20.97	4.85	0.09	20.53	2.65	0.38
E7	5	5	4.02	19.60	0.00	4.90	2.00	0.51
E7	10	20	19.72	1.40	2.27	19.55	2.25	1.08
E8	5	20	20.55	2.75	1.94	20.37	1.85	0.79
E8	15	20	20.49	2.45	1.84	20.29	1.45	0.80

*9.41 % damage is detected at element 6 along with 11.29% damage at element 8

Total eight damage cases which constitute both single and multiple damage case are considered in this study. Similar to simply supported beam, normally distributed random noise up to 20% is added to numerically estimated curvature mode shapes to simulate experimental condition. Similar comparison for damage assessment is made using first three and first five curvature modes. All the considered damage cases and the damage assessment results are shown in Table 3. The normalized changes in curvature mode shapes for multiple damage identification case with damages at locations 5 and 10 and damage amount 10% and 15% respectively, is presented in Fig. 13.

A trend similar to previous two tables is observed in Table 3 wherein the present two stage damage identification method could successfully identify and quantify the damaged members. It is observed that, with first three modes the present algorithm has detected a false damage at location 6 in E2 damage condition whereas with first five modes it could successfully capture the same. Further, the error associated with damage quantification is significantly less in case of five modes. Thus in conclusion, all these extensive studies show the robustness of the proposed methodology for damage assessment.

4. Conclusions

A simple but robust technique for detecting and quantifying damages in structures is presented in this paper. A two-step procedure is suggested for this purpose, where the maximum difference in curvature mode shapes of the undamaged and damaged structure is used for visual identification of probable damaged elements, and then an optimization technique called unified particle swarm optimization is used for final quantification of damages. The advantage of this two-step procedure is that it reduces the search space and hence reduces the associated computational cost and simultaneously improves the accuracy. Though the proposed procedure is demonstrated with few beam examples, it can easily be extended to identify damages in frame like structures. As indicated by the simulation results, the proposed method is able to detect and quantify the damage accurately using first three curvature mode shapes in case of single element damage case. Further, the procedure is able to assesses damages with a higher level of accuracy even in noisy environment. However, more number of curvature mode shapes will ensure its accuracy in predicting multiple damages especially in noisy environment.

Acknowledgements

This project is financially supported by Aeronautical Research and Development Board (Structures Panel), Ministry of defense (R&D), Govt. of India.

References

- Al-Ghalib, A.A., Mohammad, F.A., Rahman, M. and Chilton, J. (2011), "Damage identification in a concrete beam using curvature difference ratio", *J. Phys. Conf. Ser.*, **305**, 012109.
- Bakhary, N., Hao, H. and Deeks, A. (2010), "Structure damage detection using neural network with multi-stage substructuring", *Adv. Struct. Eng.*, **13**(1), 95-110.
- Banks, A., Vincent, J. and Anyakoha, C. (2007), "A review of particle swarm optimization. Part I:

- background and development”, *Nat. Comput.*, **6**(4), 467-484.
- Banks, A., Vincent, J. and Anyakoha, C. (2008), “A review of particle swarm optimization. Part II: hybridisation, combinatorial, multicriteria and constrained optimization, and indicative applications”, *Nat. Comput.*, **7**(1), 109-124.
- Chandrashekhar, M. and Ganguli, R. (2009), “Damage assessment of structures with uncertainty by using mode-shape curvatures and fuzzy logic”, *J. Sound. Vib.*, **326**(3-5), 939-957.
- Guo, H.Y. and Li, Z.L. (2013), “Structural damage identification based on evidence fusion and improved particle swarm optimization”, *J. Vib. Control*, DOI: 10.1177/1077546312469422.
- Kang, F., Li, J.J. and Xu, Q. (2012), “Damage detection based on improved particle swarm optimization using vibration data”, *Appl. Soft Comput.*, **12**(8), 2329-2335.
- Kang, F., Li, J.J. and Liu, S. (2013), “Combined data with particle swarm optimization for structural damage detection”, *Math. Prob. Eng.*, Article ID 416941.
- Kennedy, J. and Eberhart, R. (1995), “Particle swarm optimization”, *Proc. IEEE Int. Conf. Neural Networks*.
- Liu, H.B., Jiao, Y.B., Gong, Y.F., Bi, H.P. and Sun, Y.Y. (2011), “Damage identification for simply-supported bridge based on SVM optimized by PSO (PSO-SVM)”, *Appl. Mech. Mat.*, **80**, 490-494.
- Maity, D. and Tripathi, R.R. (2005), “Damage assessment of structures from changes in natural frequencies using genetic algorithm”, *Struct. Eng. Mech.*, **19** (1), 21-42.
- Maity, D. and Saha A. (2004), “Damage assessment in structure from changes in static parameter using neural networks”, *Sadhana*, **29**(3), 315-327.
- Majumdar, A., Maiti, D.K. and Maity, D. (2012), “Damage assessment of truss structures from changes in natural frequencies using ant colony optimization”, *Appl Math Comput*, **218**(19), 9759-9772.
- Mehrjoo, M., Khaji, N. and Ghafory-Ashtiany, M. (2013), “Application of genetic algorithm in crack detection of beam-like structures using a new cracked Euler-Bernoulli beam element”, *Appl Soft Comput*, **13**(2), 867-880.
- Nanda, B., Maity, D. and Maiti, D.K. (2012), “Vibration based structural damage detection technique using particle swarm optimization with incremental swarm size”, *J. Aeronaut. Space Sci.*, **13**(3), 323-331.
- Pandey, A.K., Biswas, M. and Samman, M.M. (1991), “Damage detection from changes in curvature mode shapes”, *J. Sound. Vib.*, **145**(2), 321-332.
- Perera, R., Fang, S.E. and Ruiz, A. (2010), “Application of particle swarm optimization and genetic algorithms to multi-objective damage identification inverse problems with modelling errors”, *Meccanica*, **45**(5), 723-734.
- Parsopoulos, K. and Vrahatis, M. (2010), *Particle Swarm Optimization and Intelligence: Advances and Applications*, IGI global, New York.
- Sahoo, B. and Maity, D. (2007), “Damage assessment of structures using hybrid neuro-genetic algorithm”, *Appl. Soft Comput.*, **7**, 89-104.
- Syedpoor, S.M. (2012), “A two stage method for structural damage detection using a modal strain energy based index and particle swarm optimization”, *Int. J. Nonlin. Mech.*, **47**(1), 1-8.
- Thatoi, D.N., Das, H. and Parhi, D.R. (2012), “Review of techniques for fault diagnosis in damaged structure and engineering system”, *Adv. Mech. Eng.*, 327569, doi:10.1155/2012/327569.
- Tripathi, R.R. and Maity, D. (2004), “Damage assessment of structure from changes in curvature damage factor using neural network”, *Ind. J. Eng. Mat. S.*, **11**, 369-377.
- Vallabhaneni, V. and Maity D. (2011), “Application of radial basis neural network on damage assessment of Structures”, *Proc. Eng.*, **14**: 3104-3110.
- Yu, L. and Xu, P. (2011), “Structural health monitoring based on continuous ACO method”, *Microelectron Reliab*, **51**(2), 270-278.
- Yun, C.B., Yi, J.H. and Bahng, E.Y. (2001), “Joint damage assessment of framed structures using a neural networks technique”, *Eng. Struct.*, **23**(5), 425-435.
- Zhang, J., Peng, H., You, C.H., Deng, Y.L. and Zhang H.Y. (2011), “Damage detection of plane member structures based on modal curvature difference method”, *Adv. Mat. Res.*, **163**, 2848-2851.